TÜBİTAK

Turkish Journal of Chemistry

http://journals.tubitak.gov.tr/chem/

Research Article

Turk J Chem
(2022) 46: 1875-1882
© TÜBİTAK
doi:10.55730/1300-0527.3487

The effect of fuel on the physiochemical properties of $ZnFe_2O_4$ synthesized by solution combustion method

Fahma RIYANTI[1], Widia PURWANINGRUM[1], Nova YULIASARI[1], Sasmita PUTRI[1], Nabila APRIANTI[2], Poedji Loekitowati HARIANI[1,*]

[1]Department of Chemistry, Faculty of Mathematics and Natural Sciences, Sriwijaya University, Indralaya, Indonesia
[2]Doctoral Program of Environmental Science, Graduate School, Sriwijaya University, South Sumatra, Indonesia

Received: 09.04.2022 • **Accepted/Published Online:** 21.07.2022 • **Final Version:** 19.12.2022

Abstract: The synthesis of $ZnFe_2O_4$ nanoparticles was performed using the solution combustion method with three types of fuel, namely urea, glycine, and ethylenediamine tetra-acetic acid (EDTA) with precursors $(Zn(NO_3)_2.6H_2O$ and $Fe(NO_3)_3.9H_2O$. The combustion process was conducted in an open space at 300 °C for ± 1 h, resulting in a brownish-black $ZnFe_2O_4$. Meanwhile, the fuel type used in the process affects the physicochemical properties of $ZnFe_2O_4$. XRD analysis showed that $ZnFe_2O_4$ synthesized using urea, glycine, and EDTA had spinel structures with crystal sizes of 10.19, 20.34, and 27.21 nm, respectively. The FTIR spectra of $ZnFe_2O_4$ synthesized using the three fuel types had Zn-O and Fe-O stretching vibrations. Furthermore, the morphology of $ZnFe_2O_4$ synthesized using urea was more homogeneous than glycine and EDTA. The saturation magnetization of $ZnFe_2O_4$ synthesized using EDTA was 54.63 emu/g compared to glycine and urea, 50.93 and 44.73 emu/g, respectively. Finally, the surface area of synthesized $ZnFe_2O_4$ using urea, glycine, and EDTA were 116.4, 100.6, and 94.2 m^2/g, respectively.

Key words: Solution combustion, $ZnFe_2O_4$, urea, glycine, EDTA, physicochemical

1. Introduction

In recent years, nanosized materials have been examined intensively. Furthermore, nanotechnology is the science of technology, referring to the ability to engineer and utilize materials as well as devices with dimensions between 1 and 100 nm [1]. Nanosized materials have unique chemical and physical properties compared to the bulk form [2]. Meanwhile, nanotechnology is becoming increasingly influential in various fields of application, ranging from the environment, to the food industry, to development even in the biomedical field, showing great potential for future clinics [3]. For example, ferrite is a magnetic nanoparticle characterized by a spinel structure with the general formula of MFe_2O_4, where M and Fe are metal cations located at the tetrahedral and octahedral sites [4]. Zinc ferrite ($ZnFe_2O_4$) is an important compound widely used in various industrial applications, such as gas sensors [5], batteries [6], catalysts [7,8], and adsorbents [9,10].

The synthesis method used influences the properties of ferrite compounds, including the size, shape, morphology, surface area, and magnetic properties [11]. Several methods of synthesizing $ZnFe_2O_4$ have been reported, including ball milling [12], coprecipitation [13,14], sol-gel [15], hydrothermal [16], and solution combustion [17]. Furthermore, this method has disadvantages, such as the formation of unwanted phases, complexity, and high cost. Therefore, a simple, easy, and low-cost technique is needed.

Solution combustion is a high-temperature synthesis that is effective and inexpensive for preparing nanomaterials such as ferrite, perovskite, and zirconia [11]. In addition, the reaction requires fast time (a few minutes) and simple equipment [18,19]. This method involves an independent reaction between an oxidizing agent (e.g., metal nitrate) as a precursor salt and a fuel (e.g., EDTA, glycine, hydrazine, urea, citric acid) [11,20]. The reactants are dissolved in water until it becomes homogeneous. Furthermore, it is heated to the boiling point of the medium, and evaporation occurs. The solution is ignited or self-ignites as the temperature rises rapidly. Simultaneously, the mixed solution changes into a fine crystalline powder of the desired composition [11]. In this process, a redox reaction or electron transfer occurs, oxidizing the fuel, and the oxidizing agent is reduced, leading to an exothermic reaction [21].

* Correspondence: puji_lukitowati@mipa.unsri.ac.id

The type of fuel used in the solution combustion affects the phase formation and morphology of the resulting nanomaterial [22]. Several fuels being used include urea, glycine, oxalyldihydrazine, carbohydrazide, EDTA, citric acid, and sucrose [23,24]. The synthesis of metal oxides using the method with several types of fuel has been examined, such as Fe_3O_4 using glycine [25], Bi_2O_3 using urea, glycine, and citric acid [26], NiO using urea and glycine [22], and $NiFe_2O_4$ using urea. [27]. Meanwhile, there is no detailed information on the suitable fuel type to synthesize specific nanomaterials. For example, the synthesis of nanomagnetic $NiFe_2O_4$ using fuel containing nitrogen (urea) produces a larger particle size than those from the hydrocarbon group [23]. This fuel type produces a variety of combustion, ranging from mild reactions that only produce mass to intense combustion reactions, which result in intense flames and explosions [28,29]. Therefore, this research aimed to explore the synthesis of $ZnFe_2O_4$ using fuel types, namely urea, glycine, and EDTA, and its effect on crystal size, magnetic properties, and surface area. The characteristics were analyzed using XRD, FTIR, SEM-EDS, and specific surface area with BET.

2. Materials and methods

2.1. Materials

The chemicals used include $Zn(NO_3)_2.6H_2O$, $Fe(NO_3)_3.9H_2O$, KCl, CH_4N_2O (urea), NH_2CH_2COOH (glycine), and $C_{10}H_{16}N_2O_8$ (EDTA), and were purchased from Merck Company. Also, distilled water was used for the experiment.

2.2. Synthesis of $ZnFe_2O_4$ Using the Solution Combustion Method

The synthesis procedure of $ZnFe_2O_4$ was as follows: 60 mL of distilled water was added to 3 beakers of 250 mL. Then, 0.5 M HNO_3 was slowly added until it reached pH 4. A total of 3.336 g Glycine, 4.0 g Urea, and 5.844 g EDTA were added to each beaker, 2.975 g of $Zn(NO_3)_2.6H_2O$ was added and stirred slowly for 10 min. Furthermore, 8.080 g of $Fe(NO_3)_3.9H_2O$ and 1.4919 g KCl were added in quantity. The mixture was homogenized using a stirrer for 15 min at room temperature. Continuously, it was stirred with a magnetic stirrer at 300 °C. After the solution changed color and the combustion process occurred, the stirring was stopped. It was further heated at 300 °C until a complete combustion reaction (±1 h). Finally, the resulting product was powder, washed with 200 mL of boiling distilled water, and dried in an oven at 80 °C for 1 h.

2.3. $ZnFe_2O_4$ characterization

The crystal structure and phase were analyzed using an X-ray diffractometer (XRD Shimadzu 7000 diffractometer) at Cu-Kα radiation = 1548 Å and range 2θ = 10–80°. The following Debye Scherrer equation (Eq. 1) was used to determine crystal size [30]:

$$D = \frac{k\lambda}{\beta \cos\theta}, \quad (1)$$

where D is the average crystal size of $ZnFe_2O_4$, λ is the X-ray wavelength (0.15418 nm), k is the Scherrer constant (0.9), β is full width at half maximum (FWHM), and θ is the Bragg diffraction angle.

The functional groups were analyzed using Fourier transform infrared (FT-IR Prestige 21 Shimadzu) at a wavenumber of 500–4000 cm^{-1}. Meanwhile, magnetic properties were analyzed using a vibrating sample magnetometer (VSM Lakeshore 74004) at room temperature, and the surface area was analyzed using the ASAP 2020.

3. Results and discussion

Figure 1 shows the synthesized $ZnFe_2O_4$ using the solution combustion method with various fuel types, namely urea, glycine and EDTA. The reaction product is a brownish-black $ZnFe_2O_4$ powder as well as H_2O, CO_2, and N_2 gases. The following shows the reaction of $ZnFe_2O_4$ synthesis using urea, glycine, and EDTA as fuel:

$3Zn(NO_3)_2.6H_2O + 6Fe(NO_3)_3.9H_2O + 20(NH_2)_2CO \rightarrow 3ZnFe_2O_4 + 112H_2O + 20CO_2 + 32N_2$

$9Zn(NO_3)_2.6H_2O + 18Fe(NO_3)_3.9H_2O + 40C_2H_5NO_2 \rightarrow 9ZnFe_2O_4 + 316H_20 + 80CO_2 + 56N_2$

$Zn(NO_3)_2.6H_2O + 2Fe(NO_3)_3.9H_2O + C_{10}H_{16}N_2O_8 \rightarrow ZnFe_2O_4 + 32H_20 + 10CO_2 + 5N_2$.

Metal nitrate is often used as an oxidizing agent because it has a higher solubility (approximately 64%) than sulfate (approximately 27%) [31]. The ideal fuel needs to have a high solubility in solvents, such as water, a low decomposition temperature (below 400 °C), produce no other residual mass, and be compatible with metal nitrates. However, other solvents such as alcohol and kerosene are used [32,33]. Maximum energy is released when the reaction is in a stoichiometric state. An oxygen supply is needed to achieve complete combustion [18]. In this research, the combustion reaction was performed in an open space at 200–300 °C, with the contribution of oxygen in the atmosphere [26]. The addition of KCl reduces the crystal size and increases the surface area. The higher addition of KCl and NaCl in the synthesis of $ZnFe_2O_4$ using the solution combustion method with L-α Alanine as fuel decreases the crystal size and increases the surface area [34].

According to JCPDS No. 22-1012, $ZnFe_2O_4$ has a spinel structure, which is at 2θ = 29.97°, 35.29°, 42.91°, 56.75°, and 62.32°, where the plane index (220), (311), (400), (511), and (440) is a plane cubic (Figure 2). Therefore, the type of fuel used in the synthesis of $ZnFe_2O_4$ affects the peak intensity of the XRD spectra. Furthermore, the highest peak intensity indicating greater crystallinity was observed in $ZnFe_2O_4$ synthesized using EDTA. The crystal size of $ZnFe_2O_4$ synthesized using urea, glycine, and EDTA was 10.19, 20.34, and 27.21 nm, respectively (Table 1).

The fuel's chain length (molecular weight) affects the crystallinity, crystal size, and particle size. It is also related to the solubility and complexation of fuel. Fuels with longer molecular chains produce a large amount of gas released during the process. In addition, fuels with a larger molecular mass have more sites for metal cations' complex formation and solubility [35]. EDTA has a molecular mass (Mw = 336.21 g/mol), greater than urea (Mw = 60.05 g/mol) and glycine (Mw = 75.07 g/mol). Another factor is the bonding heat of the reaction, depending on the number of single and double bonds in the fuel. The double bond fuel, such as urea (triple), are called unsaturated bonds and are generally more reactive. Therefore, the crystal formation process occurs quicker [26,34].

Figure 3 shows the FTIR spectra of $ZnFe_2O_4$ synthesized using urea, glycine, and EDTA. The wavenumber at 3200–3600 cm^{-1} is the stretching vibration of the O-H functional group. Furthermore, the presence of this functional group is enhanced by absorption at a wavenumber of approximately 1650 $cm^{-1,}$ which is a stretch bending of O-H [36,37]. This absorption was observed in $ZnFe_2O_4$ synthesized using glycine and EDTA. Two absorption bands at wave numbers approximately 550 cm^{-1} and 430 cm^{-1} are stretching vibrations of Zn-O and Fe-O bonds, namely the tetrahedral and the octahedral sites [38]. The wavenumbers appear at 557.43 and 416.62 cm^{-1} (fuel: urea), 553.57 and 408.9 (fuel: glycine), as well as 553.57 and 410.83 cm^{-1} (fuel: EDTA). The presence of wavenumber at 1300 cm^{-1} indicates a C=O group of the remaining fuel.

Figure 4 shows the morphology of $ZnFe_2O_4$ synthesized using urea, glycine, and EDTA The morphology of $ZnFe_2O_4$ synthesized with urea fuel appears more homogeneous and has a smaller particle size than with glycine and EDTA. On the other hand, $ZnFe_2O_4$ synthesized using glycine fuel appears as large and porous crystals. The results are similar to the synthesis of Bi_2O_3 using glycine, which has an elliptical and porous structure [26,39].

Table 2 shows the percentage of elements in $ZnFe_2O_4$ due to the analysis using EDS. $ZnFe_2O_4$ synthesized using different fuel types contains the same elements, namely Zn, O, and Fe, with different percentages. Furthermore, the stoichiometric content of these elements is 27.13%, 46.33%, and 26.54%. A similar composition was observed in $ZnFe_2O_4$ synthesized using urea.

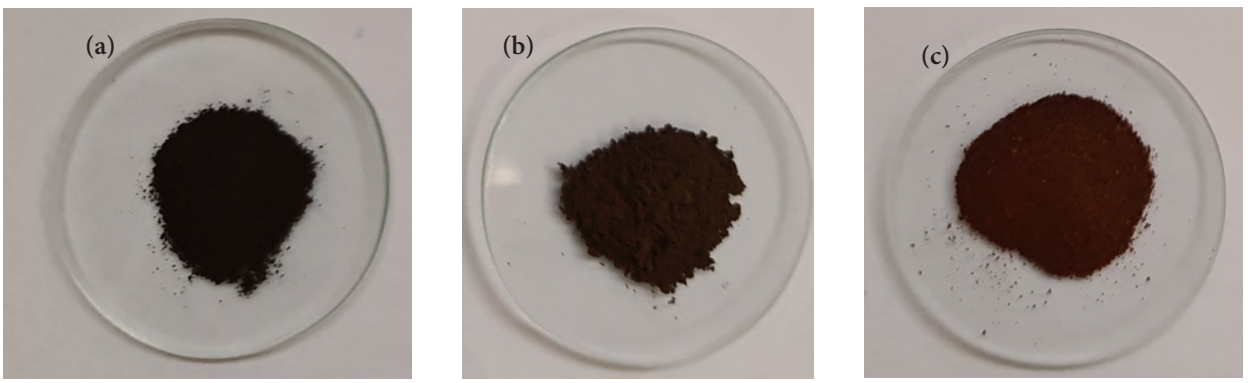

Figure 1. $ZnFe_2O_4$ synthesized using (a) urea (b) glycine and (c) EDTA.

Table 1. Data of X-ray diffraction.

Fuel	2θ (Degree)	Intensity (au)	d-spacing (Å)	Crystallite size (nm)
Urea	35.28	80.09	2.70	10.19
Glycine	35.26	318.08	2.98	20.34
EDTA	35.36	507.40	1.61	27.21

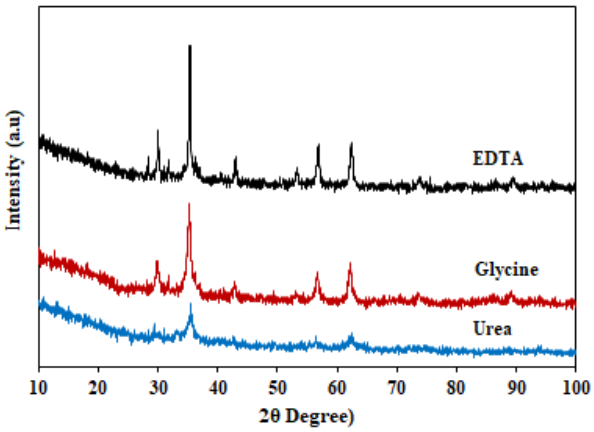

Figure 2. XRD spectra of $ZnFe_2O_4$ with fuel (a) urea (b) glycine (c) EDTA.

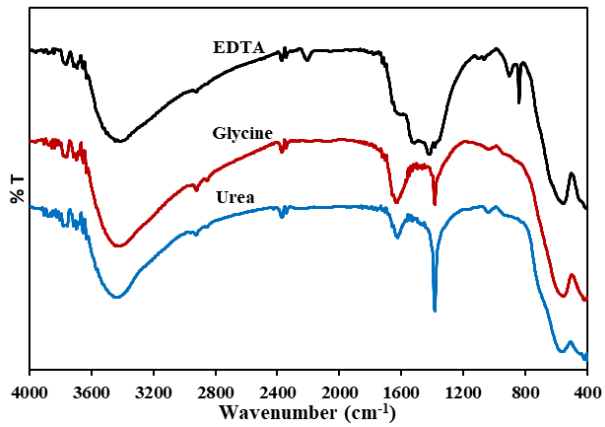

Figure 3. Spectra FTIR of $ZnFe_2O_4$ synthesized using (a) urea, (b) glycine, (c) EDTA.

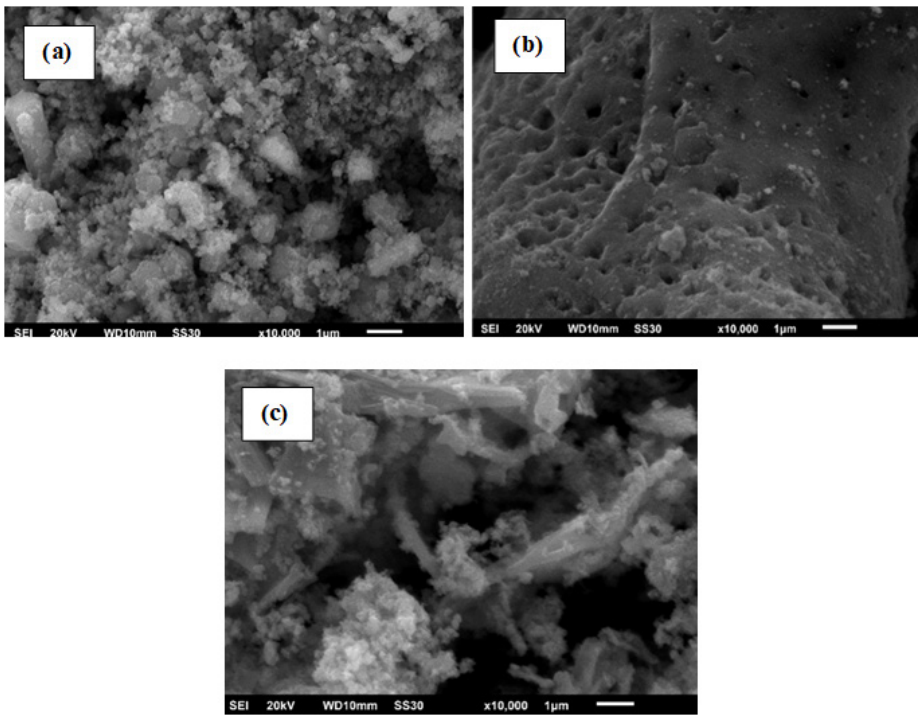

Figure 4. The morphology of $ZnFe_2O_4$ synthesized using (a) urea, (b) glycine, and (c) EDTA.

Table 2. Elements of $ZnFe_2O_4$.

Fuel	Zn (%)	Fe (%)	O (%)
Urea	26.89	46.55	25.56
Glycine	28.97	44.70	25.33
EDTA	30.16	43.55	25.29

The surface area affects the increase and decrease in the magnetic properties of nanoparticles. For example, it was reported that the magnetization of the oxide nanoparticles decreases in direct proportion to the particle size [40]. In contrast, the magnetization of some metal (cobalt) nanoparticles were reported to increase directly to particle size [41]. The decrease in magnetization of oxide nanoparticles is caused by the presence of a magnetic dead layer on the particles' surface due to the spin-glass-like behavior [40].

The nanoparticle synthesis method is essential in determining the shape, particle size, size distribution, and surface chemistry of the particles, thereby determining their magnetic properties [42,43]. In this research, $ZnFe_2O_4$ synthesized using urea, glycine, and EDTA had saturation magnetization of 44.72, 50.93, and 54.63 emu/g, respectively, proportional to the particle size (Figure 5). According to Li et al.'s [18] study on the synthesis of Fe_3O_4, the values of coercivity (Hc), remanent magnetization (Mr), and saturation magnetization (Ms) increased with increasing particle size to a maximum value which later becomes constant or decreased. Therefore, there should be a good balance between effective surface area and satisfactory magnetic performance [18,44]. When the nanoparticle size is small enough, it has superparamagnetic properties and responds mainly to the applied magnetic field [45].

Another research showed that $ZnFe_2O_4$ synthesized using the solvothermal method at various times resulted in increased crystal size and increased magnetic properties [46]. Table 3 shows the results of surface area measurements of $ZnFe_2O_4$ synthesized using urea, glycine, and EDTA of 116.4, 100.6, and 94.2 m^2/g, respectively. $ZnFe_2O_4$ synthesized using urea has the largest surface area of glycine and EDTA fuels.

Figure 6 shows a TEM image of $ZnFe_2O_4$ synthesized using urea. It appears that the particle size of ZnFe2O4 is slightly agglomerated. The particle size is between 10 and 20 nm, according to the results of calculations using XRD. Differences in particle size distribution can occur due to nonuniform heat during the combustion process.

Table 3. Crystallite size, surface area, and magnetic properties of $ZnFe_2O_4$ synthesized using several methods.

Synthesis method	Size (nm)	Surface area (m^2/g)	Ms (emu/g)	Reference
Solid state method (ZnO, Fe_2O_3) variation calcination 900–1200 °C	51.9, 52.5, 53.0, and 53.4	-	-	[47]
Solution combustion (ratio: Zn: Fe: glycine= 1: 2:1.5)	15	40.3	11.9	[39]
Coprecipitation, $ZnSO_4.7H_2O$, $FeSO_47H_2O$, and $FeCl_3$	20	-	-	[48]
Lawsonia inermis leaf extract $(Zn(CH_3COO)_2.2H_2O$ and $Fe(NO_3)_3.9H_2O$	17.12	-	42.93	[38]
Solution combustion ($Fe(NO_3)9H_2O$, $Zn(NO_3)_26H_2O$, aspartic acid, pH 10)	43	30.6		[49]
Solution combustion (ratio Zn:Fe = 1:2, triethylamine hydrochloride = 0.8, 1.0, 1.2, 1.4)	21; 25.4; 21.9 and 18.6	-	-	[50]
Coprecipitation (ZnO, Fe_2O_3 with variation sintering time (1.5, 2.5, and 3.5 h)	84.72; 70.58 and 84.72		1.12, 1.15, and 52.52	[51]
Moringa oleifera exctract ($Fe(NO_3)9H_2O$, $Zn(NO_3)_26H_2O$), annealed at 500 and 700 °C for 2 h	12.393, 16.076	-		[52]
Sol-gel method ($FeCl_3{\cdot}6H_2O$, $ZnCl_2$) with solvent EG, time reaction 2, 4 and 6 h	11.6. 16.2 and 20.5 nm		49.3, 53.8, and 61.3	[46]
Solution combustion (urea, glycine and EDTA)	10.19; 26.15 and 27.16	116.44, 100.6, and 94.2	44.74, 50.93 and 54.63	In this study

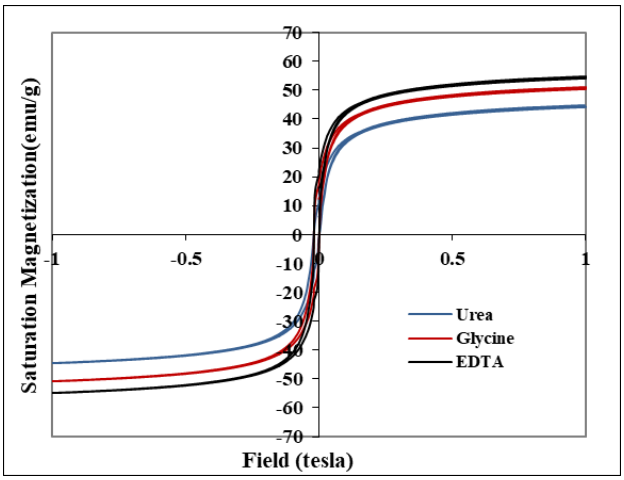

Figure 5. Magnetization curve of $ZnFe_2O_4$ synthesized using (a) urea, (b) glycine, and (c) EDTA.

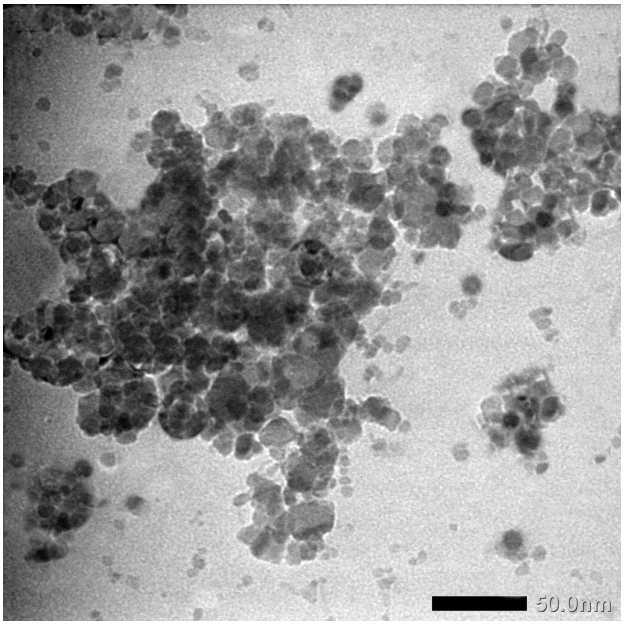

Figure 6. TEM image of $ZnFe_2O_4$ synthesized using urea.

4. Conclusion

The synthesis of $ZnFe_2O_4$ using the solution combustion method was conducted successfully. The several types of fuel used, namely urea, glycine, and EDTA, affected the physicochemical properties of the resulting $ZnFe_2O_4$, which is characterized by a spinel structure. $ZnFe_2O_4$ synthesized using urea fuel has the smallest crystallite size and magnetic properties of 10.19 nm and 44.74 emu/g, but the largest surface area is 116.4 m^2/g. Finally, the morphology of $ZnFe_2O_4$ synthesized using urea fuel appears to be more homogeneous than glycine and EDTA. The particle size of $ZnFe_2O_4$ was synthesized using urea in the range of 10–20 nm. These characteristics of $ZnFe_2O_4$ have the potential to be applied as adsorbent, catalyst and biomedical.

Acknowledgment

This project was funded by the DIPA of Public Service Agency of Sriwijaya University 2021 (SP DIPA-023.17.2.677515/2021 on November 23, 2020; in accordance with the Rector's Decree Number: 0007/UN9/SK.LP2M.PT/2021) in SATEKS scheme.

References

1. Pop D, Buzatu R, Moaca EA, Watz CG, Pinzaru SC et al. Development and characterisation of Fe_3O_4@carbon nanoparticles and their biological screening related to oral administration. Materials 2021; 14: 1-24. doi: 10.3390/ma14133556.
2. Martin CR. Nanomaterials: A Membrane-Based Synthetic Approach. Science 1994; 266 (5193): 1961-1966. doi: 10.1126/science.266.5193.1961
3. Beloqui A, Solins MA, Rodrigues-Gascon A, Almeida AJ, Preat V. Nonostructure lipid carriers: promising drug delivery system for future clinics. Nanomedicine 2016; 12 (1): 143-161. doi: 10.1016/j.nano.2015.09.004
4. Amulya MAS, Nagaswarupa HP, Kumar MRA, Ravikumar CR, Prashanta SC et al. Sonochemical synthesis of $NiFe_2O_4$ nanoparticles: characterization and their photocatalytic and electrochemical applications. Applied Surface Science Advances 2020; 1 (1): 1-10. doi: 10.1016/j.apsadv.2020.100023
5. Zhou X, Liu J, Wang C, Sun P, Hua X et al. Highly sensitive acetone gas sensor based on porous $ZnFe_2O_4$. Sensors and Actuators B: Chemical 2015; 206: 577-583. doi: 10.1016/j.snb.2014.09.080
6. Thankachan RM, Rahman Md M, Sultana I, Glushenkov AM, Thomas S et al. Enhanced lithium storage in $ZnFe_2O_4$–C nanocomposite produced by a low-energy ball milling. Journal of Power Sources 2015; 282: 462-47. doi: 10.1016/j.jpowsour.2015.02.039

7. Mahmoodi NM. Zink ferrite nanoparticle as a magnetic catalyst: synthesis and dye degradation. Materials Research Bulletin 2013; 48: 4255-4260. doi: 10.1016/j.materresbull.2013.06.070.

8. Choi YH, Ra EC, Kim EH, Kim KY, Jang YJ et al. Sodium-containing spinel zinc ferrite as a catalyst precursor for the selective synthesis of liquid hydrocarbon fuels. ChemSusChem 2017; 10 (23): 4764-4770. doi: 10.1002/cssc.201701437.

9. Qiang WG, Chao XM, Wu XD. Enhanced adsorption of phosphate onto zinc ferrite by incorporating cerium. Chemical Engineering Research and Design 2017; 117: 706-714. doi: 10.1016/j.cherd.2016.11.026.

10. Wu C, Xu Y, Xu S, Tu J, Tian C et al. Enhanced adsorption of arsenate by spinel zinc ferrite nano particles: Effect of zinc content and site occupation. Journal of Environmental Sciences 2019; 79: 248-255. doi: 10.1016/j.jes.2018.09.010.

11. Deshpande K, Mukasyan A, Varma A. Direct synthesis of iron oxide nanopowders by the combustion approach: reaction mechanism and properties. Chemistry of Materials 2004; 16: 4896-4904. doi: 10.1021/cm040061m

12. Bid S, Pradha SK. Preparation of zinc ferrite by high-energy ball-milling and microstructure characterization by Rietveld's analysis. Materials Chemistry and Physic 2003; 82 (1): 27-37. doi: 10.1016/S0254-0584(03)00169-X

13. Ebrahimi M, Shahraki RR, Ebrahimi SAS. Magnetic properties of zinc ferrite nanoparticles synthesized by coprecipitation method. Journal of Superconductivity and Novel Magnetism 2014; 27: 1587-1592. doi: 10.1007/s10948-014-2485-4.

14. Linma ES, Coasta LS, Sampaio GRLM, Oliveira ES, Silva EB et al. Zinc ferrite nanoparticles via coprecipitation modified method: glycerol as structure directing and stabilizing agent. Journal of the Brazilian Chemical Society 2019; 30 (4): 882-891. doi: 10.21577/0103-5053.20180225.

15. Kido Y, Nakanishi K, Kanamoria K. Sol–gel synthesis of zinc ferrite-based xerogel monoliths with well-defined macropores. RSC Advances 2013; 3: 3661-3666. doi: 10.1039/C3RA22481C.

16. Coppola P, da Silva FG, Gomide G, Paula FLO, Campos AFC et al. Hydrothermal synthesis of mixed zi. nc–cobalt ferrite nanoparticles: structural and magnetic properties. Journal of Nanoparticle Research 2016; 18: 138. doi: 10.1007/s11051-016-3430-1.

17. Bera P, Lakshmi RV, Prakash BH, Tiwari K, Shukla A et al. Solution combustion synthesis, characterization, magnetic, and dielectric properties of $CoFe_2O_4$ and $Co0.5M0.5Fe_2O_4$ (M = Mn, Ni, and Zn). Physical Chemistry Chemical Physics 2020; 35: 20087-200106. doi: 10.1039/D0CP03161E.

18. Li FT, Ran J, Jaroniec M, Qiao SZ. Solution combustion synthesis of metal oxide nanomaterials for energy storage and conversion. Nanoscale 2015; 7 (42): 17590–17610. doi: 10.1039/C5NR05299H

19. Rani R, Dhiman P, Sharma SK, Singh M. Structural and magnetic studies of $Co0.6Zn0.4Fe_2O_4$ nanoferrite synthesized by solution combustion method. Synthesis and Reactivity in Inorganic, Metal-Organic, and Nano-Metal Chemistry 2012; 42 (3): 360-363. doi: 10.1080/15533174.2011.611062

20. Qrtiz-Quinonez JL, Pal U, Villanueva MS. Structural, magnetic, and catalytic evaluation spinel Co, Ni and Co-Ni ferrite nanoparticles fabricated by low-temperature. ACS Omega 2018; 3: 14986-15001. doi: 10.1021/acsomega.8b02229

21. Carlos E, Martins R, Fortunato E, Branquinho R. Solution combustion synthesis: towards a sustainable approach for metal oxides. Chemistry - A European Journal 2020; 26 (42): 9099-9125. doi: 10.1002/chem.202000678

22. Raveendra RS, Prashanth PA, Nagabhushana BM. Study on the effect of fuels on phase formation and morphology of combustion derived α-Al_2O_3 and NiO nanomaterials. Advanced Materials Letters 2016; 7 (3): 216-220. doi: 10.5185/amlett.2016.6202

23. Lazarova T, Georgieva M, Tzankov D, Voykova D, Aleksandrov L et al. Influence of the type of fuel used for the solution combustion synthesis on the structure, morphology and magnetic properties of nanosized $NiFe_2O_4$. Journal of Alloys and Compounds 2017; 700: 272-283. doi: 10.1016/j.jallcom.2017.01.055

24. Karakas ZK, Boncukcuoglu R, Karakas IH. The effects of fuel type in synthesis of $NiFe_2O_4$ nanoparticles by microwave assisted combustion method. Journal of Physics: Conference Series 2016; 707: 1-11. doi: 10.1088/1742-6596/707/1/012046

25. Mukasyan AS, Epstein P, Dinka P. Solution combustion synthesis of nanomaterials. Proceedings of the Combustion Institute 2007; 31: 1789-1795. doi: 10.1016/j.proci.2006.07.052

26. Astuti Y, Amri D, Widodo DS, Widiyandari H, Balgis R et al. Effect of fuels on the physicochemical properties and photocatalytic activity of bismuth oxide, synthesized using solution combustion method. International Journal of Technology 2020; 11 (1): 26-36. doi: 10.14716/ijtech.v11i1.3342

27. Hariani PL, Said M, Rachmat A, Riyanti F, Pratiwi HC et al. Preparation of $NiFe_2O_4$ nanoparticles by solution combustion methods as photocatalyst of Congo Red. Bulletin of Chemical Reaction Engineering & Catalysis 2021; 16 (3): 481-490. doi: 10.9767/bcrec.16.3.10848.481-490.

28. Ding J, Liu XY, Wang J, Shi Y. Ultrafine ferrite particles prepared by coprecipitation/mechanical milling. Materials Letters 2000; 44: 19-22. doi: 10.1016/S0167-577X(99)00290-6.

29. Patil KC, Aruna ST, Mimani, T. Combustion synthesis: an update. Current Opinion in Solid State and Materials Science 2002; 6 (6): 507-512. doi: 10.1016/S1359-0286(02)00123-7

30. Lin CC, Ho JM. Structural analysis and catalytic activity of Fe_3O_4 nanoparticles prepared by a facile co-precipitation method in a rotating packed bed. Ceramics International 2016; 40: 10275-10282. doi: 10.1016/j.ceramint.2014.02.119.

31. Varma A, Mukasyan AS, Rogachev AS, Manukyan KV. Solution combustion synthesis of nanoscale materials. Chemical Reviews 2016; 116: 14493-14586. doi: 10.1021/acs.chemrev.6b00279.

32. Tani T, Watanabe N, Takatori K, Pratsinis SE. Morphologies of oxide particles made by the emulsion combustion method. Journal of the American Ceramic Society 2003; 86: 898-904. doi: 10.1111/j.1151-2916.2003.tb03394.x

33. Illic S, Zec S, Miljkovic M, Poleti D, Markovic MP et al. Sol gel synthesis and characterization of iron doped mullite. Journal of Alloys and Compounds 2014; 612: 259-264. doi: 10.1016/j.jallcom.2014.05.204

34. Yang J, Li X, Deng X, Huang Z, Zhang Y. Salt-assisted solution combustion synthesis of $ZnFe_2O_4$ nanoparticles and photocatalytic activity with TiO_2 (P25) as nanocomposite. Journal of the Ceramic Society of Japan 2012; 120: 579-583. doi: 10.2109/jcersj2.120.579

35. Novitskaya E, Kelly JP, Bhaduri S, Graeve OA. A review of solution combustion synthesis: an analysis of parameters controlling powder characteristics. International Materials Reviews 2021; 66 (3): 188-214. doi: 10.1080/09506608.2020.1765603

36. Silvestein RM, Webster FX, Kiemle DJ, Bryce DL. Spectrometric identification of organic compounds, Wiley 2014, New York.

37. Kurian J, Mathew MJ. Structural, optical and magnetic studies of $CuFe_2O_4$, $MgFe_2O_4$ and $ZnFe_2O_4$ nanoparticles prepared by hydrothermal/solvothermal method. Journal of Magnetism and Magnetic Materials 2018; 451: 121-130. doi: 10.1016/j.jmmm.2017.10.124

38. Sarala E, Naik MM, Vinuth M, Reddy YVR, Sujatha HR. Green synthesis of Lawsonia inermis-mediated zink ferrite nanoparticles for magnetic studies and anticancer activity against breast cancer (MCF-7) cell lines. Journal of Materials Science: Materials in Electronics 2020; 31: 8589-8596. doi: 10.1007/s10854-020-03394-8

39. Xue H, Li Z, Wang X, Fu X. Facile synthesis of nanocrystalline zinc ferrite via a self-propagating combustion method. Materials Letters 2007; 61: 347-350. doi: 10.1016/j.matlet.2006.04.061

40. Kodama RH. Magnetic nanoparticles. Journal of Magnetism and Magnetic Materials 1999; 200: 359-372. doi: 10.1016/S0304-8853(99)00347-9

41. Respaud M, Broto JM, Rakoto H, Fert AR, Thomas L et al.Surface effects on the magnetic properties of ultrafine cobalt particles. Physical Review B 1998; 57: 2925–2935. doi: 10.1103/PhysRevB.57.2925

42. Kouhi M, Vahedi A, Akbarzadeh A, Hanifehpour Y, Joo SW. Investigation of quadratic electro-optic effects and electroabsorption process in GaN/AlGaN spherical quantum dot. Nanoscale Research Letters 2014; 9: 131–136. doi: 10.1186/1556-276X-9-131

43. Koo KN, Ismail AF, Othman MHD, Rahman MA, Sheng TZ. Preparation and characterization of superparamagnetic magnetite (Fe_3O_4) nanoparticles: A short review. Malaysian Journal of Fundamental and Applied Sciences 2019; 15 (1): 23-31. doi: 10.11113/mjfas.v15n2019.1224

44. Issa B, Obaidat IM, Albiss BA, Haik Y. Magnetic nanoparticles: surface effects and properties related to biomedicine applications. International Journal of Molecule Sciences 2013; 14: 21266-21305. doi: 10.3390/ijms141121266

45. Ghazanfari MR, Kashefi M, Shams SF, Jaafari MR. Perspective of Fe_3O_4 nanoparticles role in biomedical applications. Biochemistry Research International 2016; 1-32. doi: 10.1155/2016/7840161

46. Guo P, Cui L, Wang Y, Lv M, Wang B et al. Facile synthesis of $ZnFe_2O_4$ nanoparticles with tunable magnetic and sensing properties. Langmuir 2013; 29: 8997-9003. doi: 10.1021/la401627x

47. Jang JS, Hong SJ, Lee JS. Synthesis of zink ferrite and its photocatalytic application under visible light. Journal of the Korean Physical Society 2009; 54 (1): 204-208. doi: 10.3938/jkps.54.204

48. Kumar GSY, Naik HSB, Roy AS, Harish KN, Viswanath R. Synthesis, optical and electrical properties of $ZnFe_2O_4$ nanocomposites. Nanomaterial and Nanotechnology 2012; 2: 1-6. doi: 10.5772/56169

49. Shanmugavani A, Selvan RK. Synthesis of $ZnFe_2O_4$ nanoparticles and their asymetric configuration with $Ni(OH)_2$ for a pseudocapacitor. RSC advances 2014; 4: 27022-27029. doi: 10.1039/C4RA01793E

50. Liu RH, Li FT. Facile combustion synthesis of $ZnFe_2O_4$ for photocatalytic oxidative desulfurization of thiophene in model oil. International Journal of Petroleum Technology 2017; 4: 24-27. doi: 10.15377/2409-787X.2017.04.4

51. Puspitasari P, Rizkia UA, Sukarni S, Permanasari AA, Taufiq A et al. Effects of various sintering conditioning on the structural and magnetic properties of zink ferrite ($ZnFe_2O_4$). Material Research 2021, 24 (1): 1-5. doi: 10.1590/1980-5373-MR-2020-0300

52. Matinise N, Kaviyarasu K, Mongwaketsi N, Khamlich S, Kotsedi L et al. Green synthesis of novel zink iron oxide ($ZnFe_2O_4$) nanocomposite via Moringa Oleifera natural extract for electrochemical applications. Applied Surface Science 2018; 446: 66-73. doi: 10.1016/j.apsusc.2018.02.187